

Modeling Primary Blast Injury in Isolated Spinal Cord White Matter

Sean Connell, B.S., ²Hui Ouyang, B.S. ^{1,2} and Riyi Shi, M.D., Ph.D. ^{1,2}

¹Department of Basic Medical Sciences, ²Weldon School of Biomedical Engineering
Purdue University,
West Lafayette, Indiana, USA
riyi@purdue.edu

Abstract - Primary blast injury (PBI) is a common injury associated with present military conflicts and leads to significant neurological deficits. In order to prevent and treat this injury, an appropriate understanding of the biological response is required. A blast wave generator was created as an experimental model to elucidate this response by creating a repeatable blast injury on ex-vivo guinea pig spinal cord white matter. Subsequently, this study defines approximate limits for blast force and provides a relationship between axonal damage, nerve conduction parameters and functional recovery. Action potential generation and physical deficits of spinal cords exposed to blast injury were measured using a double sucrose gap-recording chamber and a dye-exclusion assay. Results express an inverse correlation between the severity of blast injury and degree of recovery. Such an approach is expected to contribute significantly to the detection and prediction of functional deficits by providing a critical analysis of nerve damage in order to effectively devise and implement repair techniques for PBI.

Keywords – Blast Injury, CNS, Spinal Cord Injury

I. INTRODUCTION

Blast-induced neurotrauma is a common injury modality associated with the current war efforts and increasing levels of terrorist activity [1-3]. Exposure to the primary pressure wave generated by explosive devices causes significant neurological deficits and is responsible for many of the war related pathologies during Operation Iraqi Freedom and the Global War on Terror. PBI in the central nervous system (CNS) causes neuronal death and leads to decreased neurological function. Following the initial impact trauma, the secondary biochemical response associated with neurotrauma, such as the production of free radicals and the increased expression of acrolein (a known neuronal toxin), further degrades the injury site. [4] Despite the far-reaching effects of the aforementioned debilitating disorders, the underlying mechanisms governing the functional loss associated with the CNS are poorly understood. Previously established animal models for blast injury have analyzed global responses, but lack an understanding of the physical injury and the primary and secondary response mechanisms at the tissue level [5-7]. Poor characterization of these reactions prevents adequate intervention and treatment. Therefore, appropriate

understanding of the mechanisms involved in blast injury is paramount for increasing soldier survivability and treating afflicted individuals.

The current study introduces several novel *ex vitro* techniques to model the effects of PBI in an attempt to elucidate the mechanisms of blast injuries on the CNS, particularly in relation to spinal cord tissue. For this study, a blast wave generator was created to model an improvised explosion in order to create a reproducible and controllable degree of injury for analysis. Functional and anatomical deficits resulting from blast exposure will be continuously monitored using an electrophysiological recording apparatus to characterize neurological activity and a dye-exclusion assay to quantify axonal membrane integrity.

II. MATERIALS AND METHODS

A. Isolation of Spinal Cord White Matter

The experimental protocol used for this study was approved by the Purdue University Animal Care and Use Committee. Twelve guinea pigs, weighing between 250g and 350g were anesthetized (ketamine 60 mg/kg and xylazine 10 mg/kg) prior to perfusion with cold oxygenated Kreb's solution (124mM NaCl, 5mM KCl, 1.2mM KH₂PO₄, 1.3mM MgSO₄, 2mM CaCl₂, 20mM dextrose, 26mM NaHCO₃ and 10 mM sodium ascorbate). The vertebral column was removed and the spinal cord ventral white matter was carefully excised by cutting through the pedicles longitudinally along the column similar to previously described techniques and shown diagrammatically in Figure 1A [8-11]. Prior to testing, the ventral white matter was allowed to recover and equilibrate in continuously oxygenated Kreb's solution for at least one hour.

B. Blast Induced Injury

The primary blast injury was created using a novel blast generator. One-inch sections of shock tubing (NONEL Lead Line with an explosive lining of 0.1 grains/foot composed of tetrinitramine (HMX) and aluminium) housed in a hollow aluminum blast nozzle approximately 6 inches in length was detonated with a remote initiator (Wizard Shock Tube Initiator plasma discharge device). Excised sections of spinal cord

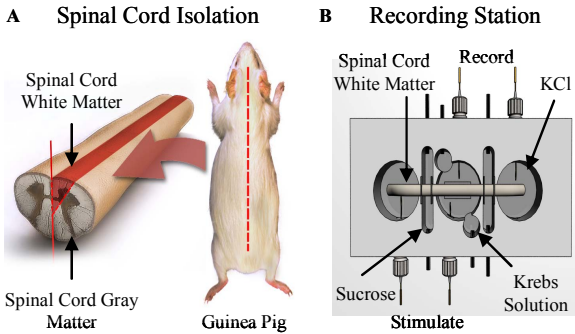


Figure 1: (A) Spinal cord extraction and isolation of ventral white matter (B) Double sucrose gap recording chamber (top view) and spinal cord segment depicting stimulus application on the left side and recording of evoked CAPs on the right.

white matter were secured in the double sucrose gap chamber directly beneath the blast nozzle for continuous monitoring of electrophysiological function. Varying degrees of blast injury were created by calibrating the distance between the spinal cord section and the blast nozzle for three primary injury levels. The Low levels of blast injury occurred at a distance of 1.75cm, followed by a Medium exposure at 1.5cm and finally a High degree of blast injury at 1.25cm. Overpressure values for each injury level were determined independently using a dynamic pressure transducer (DPX101 by Omega) mounted normal to the propagating pressure wave.

B. Electrophysiological Recording

Electrophysiological function of excised spinal cords was continuously monitored before and after exposure to a blast injury using a double sucrose gap-recording chamber. (Fig. 1B) Ventral white matter strips were placed across the chamber with the middle of the cord housed in the central compartment under constant perfusion of oxygenated Kreb's solution maintained at 37°C, while either end of the cord rested in the side compartments containing isotonic KCl (120mM). Both gaps separating the side compartments from the central portion were perfused with sucrose (320mM) to avoid ion exchange. One end of the cord was stimulated with a 0.3V constant voltage pulse every 3 sec and the corresponding CAPs were recorded from the distal end using Ag-AgCl electrodes. A detailed description of the construction and dimensions of the chamber are reported in previous studies [8-11].

C. Membrane Integrity and HRP Analysis

The HRP exclusion assay was performed as previously described to quantify the degree of membrane damage [8-11]. Immediately following exposure to blast injury, the ventral white matter strips were transferred into an oxygenated Kreb's solution containing 0.015% HRP for one-hour before being placed in a 2.5% glutaraldehyde solution in phosphate buffer for two-hours. Treated spinal cords were then cut into 30 μm transverse sections at the center of the injury site using a vibratome. Sections were processed with diaminobenzidine

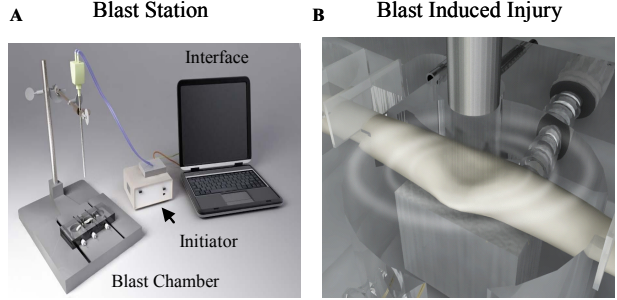


Figure 2: (A) Blast station consisting of the computer interface, initiator for detonation and blast chamber containing the recording station and shock tubing housed within the blast nozzle. (B) Detailed view of primary blast wave impacting the excised section of spinal cord ventral white matter within the recording chamber.

(DMB) to visualize the degree of HRP uptake in damaged axons. Digital images of HRP-stained sections were used to quantify the total number of stained axons and results are reported as a mean density (axons/mm²).

D. Statistical Analysis

Statistical significance was determined using one-way ANOVA. Subsequent comparisons were performed using a Tukey test with significance level of $P < 0.05$. Values are reported as means \pm standard error.

III. RESULTS

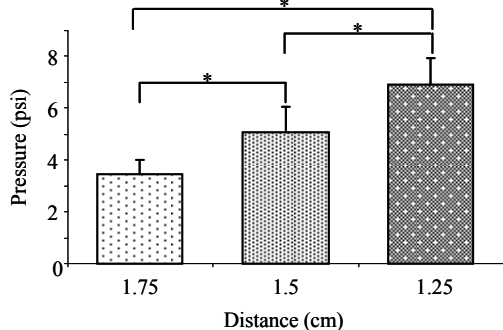
A. Blast Induced Injury

Peak pressure was calibrated as a function of distance from the ventral white matter segment to produce three distinct levels of blast injury. Implementing each blast injury level revealed significant correlations between the degree of injury, membrane damage and subsequent functional loss. Resulting peak pressure values are shown in Figure 2A above. The three significantly different blast modalities were designated as Low at 1.75cm from the ventral white matter segment with an average peak pressure of $3.45 \pm 0.55\text{psi}$, followed by Medium exposure (1.5cm at $5.09 \pm 0.97\text{psi}$) and finally a High exposure level (1.25cm at $6.89 \pm 1.04\text{psi}$). Representative pressure-time histories for blast waves created for each injury level are also depicted in Figure 2B, illustrating the varying magnitudes of blast injury and the sharp increase in overpressure following detonation. Peak overpressure is followed by subsequent oscillations between negative and positive phases. Minimal fluctuations in the sinusoidal pressure wave following the initial detonation of the shock tubing is attributed to the equilibration of the force plate on the pressure transducer.

B. Electrophysiological Recording

Loss of neurological function was correlated with electrophysiological deficits by continuously monitoring CAP amplitudes using the double sucrose gap-recording chamber. Percent reduction in CAP amplitudes for each pressure level was determined by comparing pre- and post-blast amplitudes,

A Overpressure Varies with Distance



B Blast Wave

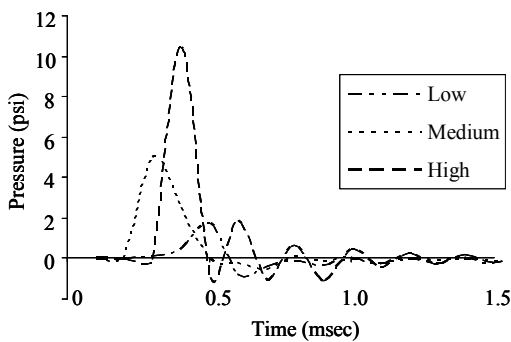


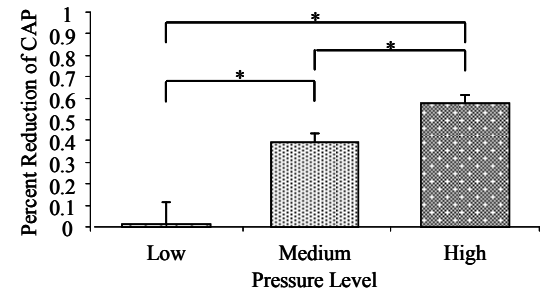
Figure 3: (A) Peak pressure outputs for the three degrees of blast injury ($p < .05$), $n = 8$ (B) Representative pressure-time history for blast waves projected from each injury level (Low, Medium and High) depicting the sharp increase in overpressure and characteristic waveform.

as reported in Figure 4A. Increasing pressure levels resulted in a significant increase in amplitude reduction ranging from $1 \pm 1\%$ reduction for Low blast injuries to $39.1 \pm 4.4\%$ for the Medium level injury, up to $57.9 \pm 3.5\%$ reduction for High exposure. Application of the increasing levels of blast force reveal and inverse correlation with respect to CAP amplitudes. Subsequent plots in Figure 4B demonstrate the reduction in amplitude following exposure to a medium level blast injury. No significant change in latency was detected (values not reported).

C. Membrane Integrity and HRP Analysis

Anatomical damage was quantified using an HRP-exclusion assay to visualize damaged axons in the spinal cord sections exposed to each level of blast injury. A significant difference between treatment groups was found in comparison to the High level of injury, but no significant differences between Medium and Low injury levels were recorded. Exposure to a high-level blast injury damaged 2916.45 ± 646.39 axons/mm², followed by a medium exposure at 631.85 ± 289.64 axons/mm² and low exposure at 35.27 ± 77.64 axons/mm². However, each injury level resulted in a significant increase in anatomical damage when compared to

A Blast Damage Impairs CAP Amplitude



B

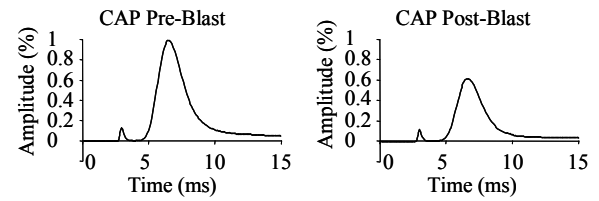


Figure 4: (A) Percent reduction in electrophysiological function by comparing baseline measurements and amplitudes of CAPS following sufficient recovery from blast injury ($p < .05$), $n = 3$ (B) Representative CAPs depicting significant reduction in amplitude of evoked CAPs after sustaining a Medium level blast injury.

an uninjured control section with 7 ± 1.7 axons/mm², as reported in Figure 5A. Similar to the reduction of CAP amplitude, anatomical damage was found to be inversely related to the degree of blast injury. Photomicrographs for injured ventral white matter sections are depicted in Figure 5B for visual comparison of injured axons to unstained healthy axons for each treatment group and the uninjured control section.

IV. DISCUSSION

The prevalence of PBI is increasing due to modern war efforts and continuing terrorist activity around the world. As a result, significant research efforts are being directed to the study of this particular and unique injury modality. Basic understanding of the injury mechanisms and pathological response of the CNS are crucial for future treatment and ultimately the prevention of traumatic blast-induced neurotrauma.

The current study expands on this research demand by creating a novel model for blast-induced neurotrauma, which can be used to elucidate the injury on a tissue level. As demonstrated throughout the study, the production of significantly different blast injury levels (i.e. Low, Medium and High) by calibrating the peak pressure produced by the blast chamber elucidated an inverse relationship between blast injury and both anatomical and functional deficits. This quantifiable relationship can be used for the future study and analysis of this injury modality in a highly specific and unprecedented degree.

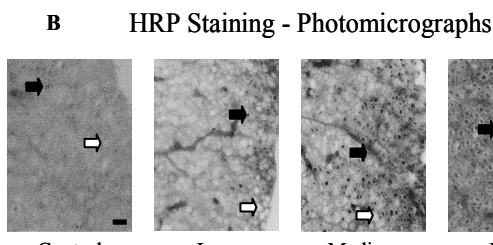
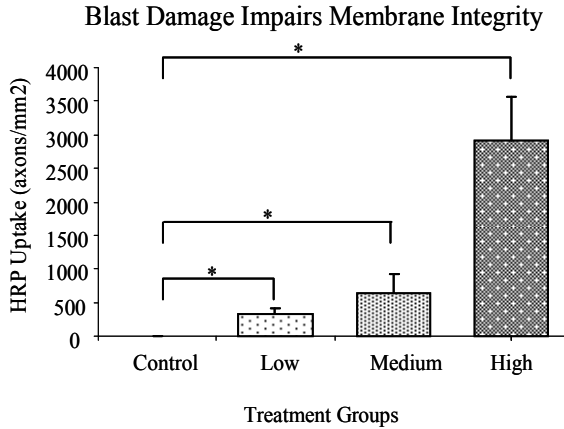


Figure 5: (A) HRP-exclusion assay for testing membrane integrity of axons for three levels of blast injury based on HRP uptake ($p < .05$), $n = 3$ (B) Representative photomicrographs of HRP stained sections. Black arrows indicate damaged axons and HRP uptake. White arrows indicate undamaged axons. Scale bar represents 10 μ m.

This *ex vivo* model will allow for rapid characterization of the injury by mitigating any confounding factors associated with *in vivo* models, a significant advantage when compared to previously established blast models. Thus, allowing for a basic understanding of the key components of blast injury.

Furthermore, this model will allow for the implementation and testing of various treatment options by creating a highly precise and reproducible blast injury. Future expansion of this model will include the global response of a blast injury *in vivo* in order to correlate immediate tissue deformation and functional loss to the global onset of symptoms associated with traumatic blast-induced neurotrauma. Future studies will also include a mechanistic approach for the prevention of blast injury in CNS by allowing for the rapid characterization of protective gear, armor or application of future preventative therapies.

V. CONCLUSION

In summary, the current investigation provides the fundamental knowledge to determine injury parameters and assess acute tissue damage of blast-induced neurotrauma. Such an approach is expected to contribute significantly to the detection, and prediction of blast trauma in the CNS. More importantly, such knowledge will facilitate the preservation of sensory, motor, and cognitive function of the victims through effective medical interventions and increase the post-injury quality of life.

ACKNOWLEDGMENT

The authors thank Michel Schweinsberg for the graphic illustrations and Mike Koppes for providing the explosives

used throughout the study. The funding for this study was partially provided by the State of Indiana and the Indiana Spinal Cord and Brain Injury Research Fund.

REFERENCES

- [1] G. J. Argyros, "Management of primary blast injury," *Toxicology*, vol. 121, pp. 105-15, 1997.
- [2] R. G. DePalma, D. G. Burris, H. R. Champion, and M. J. Hodgson, "Blast injuries," *N Engl J Med*, vol. 352, pp. 1335-42, 2005.
- [3] M. A. Mayorga, "The pathology of primary blast overpressure injury," *Toxicology*, vol. 121, pp. 17-28, 1997.
- [4] K. Hamann, A. Durkes, H. Ouyang, K. Uchida, A. Pond, and R. Shi, "Critical role of acrolein in secondary injury following ex vivo spinal cord trauma," *J Neurochem*, vol. 107, pp. 712-21, 2008.
- [5] M. Chavko, W. A. Koller, W. K. Prusaczyk, and R. M. McCarron, "Measurement of blast wave by a miniature fiber optic pressure transducer in the rat brain," *J Neurosci Methods*, vol. 159, pp. 277-81, 2007.
- [6] R. J. Irwin, M. R. Lerner, J. F. Bealer, S. A. Lightfoot, D. J. Brackett, and D. W. Tuggle, "Global primary blast injury: a rat model," *J Okla State Med Assoc*, vol. 91, pp. 387-92, 1998.
- [7] J. H. Jaffin, L. McKinney, R. C. Kinney, J. A. Cunningham, D. M. Moritz, J. M. Kraimer, G. M. Graeber, J. B. Moe, J. M. Salander, and J. W. Harmon, "A laboratory model for studying blast overpressure injury," *J Trauma*, vol. 27, pp. 349-56, 1987.
- [8] H. Ouyang, B. Galle, J. Li, E. Nauman, and R. Shi, "Critical roles of decompression in functional recovery of ex vivo spinal cord white matter," *J Neurosurg Spine*, vol. 10, pp. 161-70, 2009.
- [9] R. Shi, "The dynamics of axolemmal disruption in guinea pig spinal cord following compression," *J Neurocytol*, vol. 33, pp. 203-11, 2004.
- [10] R. Shi and R. B. Borgens, "Anatomical repair of nerve membranes in crushed mammalian spinal cord with polyethylene glycol," *J Neurocytol*, vol. 29, pp. 633-43, 2000.
- [11] R. Shi and J. Whitebone, "Conduction deficits and membrane disruption of spinal cord axons as a function of magnitude and rate of strain," *J Neurophysiol*, vol. 95, pp. 3384-90, 2006.